HHS Public Access

Author manuscript

J Immunol. Author manuscript; available in PMC 2018 November 01.

Published in final edited form as:

J Immunol. 2017 November 01; 199(9): 3202–3211. doi:10.4049/jimmunol.1700586.

Phenotypic and Functional Characterization of Circulatory, Splenic and Hepatic NK Cells in SIV controlling macaques

Diego A. Vargas-Inchaustegui[*], **Sabrina Helmold Hait**[*], **Hye-Kyung Chung**[†], **Jigna Narola**[†], **Tanya Hoang**[*], and **Marjorie Robert-Guroff**[*]

[*]Vaccine Branch, Center for Cancer Research, National Cancer Institute, National Institutes of Health, Bethesda, MD 20892

[†]Advanced BioScience Laboratories, Inc., Rockville, MD 20850

Abstract

NK cells are key components of the immune system due to their rapid response potential and their ability to mediate cytotoxic and immunomodulatory functions. Additionally, NK cells have recently been shown to persist for long periods in vivo and to have the capacity to establish immunologic memory. In the present study we studied the phenotype and function of circulatory and tissue-resident NK cells in a unique cohort of SIV controlling rhesus macaques that maintained low to undetectable levels of viremia in the chronic phase of infection. By contrasting NK responses of these macaques with those observed in SIV non-controlling and uninfected macaques we aimed to identify markers and activities of NK subpopulations associated with disease control. We show here that most differences among NK cells of the three groups of macaques were observed in tissue-resident cells. While SIV infection resulted in NK cell dysfunction, double negative NK cells, and those expressing CXCR3, NKG2D, and IL-18Rα were associated with viremia control, as was antibody-dependent cytotoxic function. Our results suggest several novel targets for therapeutic intervention.

INTRODUCTION

Natural killer (NK) cells are a highly specialized subset of lymphoid cells that possess cytotoxic and immunoregulatory potential (1, 2). In rhesus macaques, NK cells are phenotypically characterized as $CD3^{-}CD8\alpha^{+}CD159a^{+}$ lymphocytes that can be further subdivided based on their CD16 and CD56 expression levels, which creates unique subsets of circulatory and tissue-resident NK cells (3–5). NK cell functional activity is tightly controlled by a balance of inhibitory and activatory cell surface receptors (6, 7). Differential expression of these receptors generates NK cell heterogeneity and allows NK cells to respond to a wide variety of stimuli (8). Traditionally, NK cells have been considered short-lived, antigen non-specific components of the innate immune system. Despite this, recent evidence in mice, humans and non-human primates confirms that NK cells can be long-lived and are capable of exerting antigen-specific immune responses against haptens and viruses

Corresponding Author: Dr. Marjorie Robert-Guroff, National Cancer Institute, National Institutes of Health, 41 Medlars Drive, Building 41, Room D804, Bethesda, MD 20892-5065. Phone: (240) 760-6616; Fax: (240) 541-4454; guroffm@mail.nih.gov.

(9–11). While NK cells have long been characterized as bridging the innate and adaptive immune systems, recent findings suggest that NK cells may develop antigen specific responses that can be manipulated through vaccination (9,12).

NK cells play an important role in the early stages of HIV/SIV infection by producing IFN-γ and β-chemokines, which lead to direct killing of virus-infected cells, and have been proposed as a correlate of protection in highly exposed seronegative individuals (13, 14). Furthermore, when associated with HIV/SIV-specific antibodies, NK cells are capable of exerting potent antiviral responses that lead to prolonged antiviral control during different stages of infection (15–17). We have been using rhesus macaques as a model for the evaluation of novel HIV/SIV-specific vaccines and for studying cellular mechanisms associated with control of chronic SIV infection. We have previously shown that NK and $CD4^+$ T cell cooperative responses are strongly correlated with viremia control in SIV infected macaques (18). To further investigate the role of NK cells in maintaining low levels of chronic viremia as observed in SIV controlling macaques, we conducted detailed phenotypic and functional studies, including assessment of NK memory cells, in circulatory, splenic and liver-resident NK cells. We compared responses in a cohort of SIV controlling macaques to those in SIV non-controlling and naïve animals in order to identify novel phenotypic or functional markers that could potentially correlate with control of SIV infection. While long-term memory-like NK cells did not appear to play a role, we observed that DN NK cells as well as expression of CXCR3, NKG2D, and IL-18Rα, were associated with decreased chronic viremia in SIV controlling macaques. Furthermore, a greater capacity of NK cells to mediate antibody-dependent cytotoxic function was inversely correlated with necropsy viral loads in SIV-infected macaques. Overall our results suggest that unique phenotypic NK cells and functional NK cell responses observed in SIV controlling macaques are associated with lower chronic viral loads and may be utilized as novel correlates of protective immunity.

MATERIALS AND METHODS

Animals

This study used PBMCs, spleen and liver cells obtained from naïve or SIV_{mac251}-infected Indian rhesus macaques (*Macacca mulatta*). Uninfected (naïve) macaques (n = 6; 5 males, 1 female) were obtained from two previous, unpublished vaccine pilot studies, neither of which produced measurable anti-HIV or anti-SIV serum binding titers. SIV-infected animals were obtained from a previously published study that was designed to assess the immunogenicity and protective efficacy of different SIV Env immunogens (19). The SIV-infected macaques were categorized as SIV controllers (Low VL; n = 7; 2 males, 5 females) if they exhibited chronic plasma viral loads ≤ 10^4 RNA copies per ml of plasma. SIV non-controlling (High VL; n = 8; 3 males, 5 females) macaques displayed a chronic plasma viral load ≥ 10^4 RNA copies per ml of plasma. Two animals in the High VL group were part of the un-vaccinated control group in the previously described study (19). During post-infection monitoring, animals were housed at the NCI Animal Facility (Bethesda, MD) and maintained according to institutional Animal Care and Use Committee guidelines.

Plasma and tissue viral loads

SIV RNA viral loads in plasma were reported previously (19) and obtained by the NASBA technique (20, 21). Viral loads in spleen and PBMC obtained at the time of necropsy were determined as follows. RNA was purified from spleen cells and PBMC using the RNeasy Microarray Tissue Kit (Qiagen) according to the manufacturer's recommendations. Briefly, $10^5 – 10^7$ frozen PBMCs or spleen cells were dissolved in 1mL of QIAzol Lysis Reagent and 200μL of chloroform (Sigma-Aldrich). The solution was vigorously homogenized and rested for 3 min at room temperature (RT). After centrifugation at 12,000 X G for 20 min at 4 °C, the upper colorless phase containing total RNA was transferred to a RNeasy spin column (Qiagen) and the RNA was purified according to the kit instructions. Total RNA was recovered in 100μL of RNAse free water (Qiagen). The isolated cellular RNA was further purified by standard Ethanol/Sodium Acetate precipitation as described (22). Briefly, 2μL of RNA carrier (Thermofisher Scientific) and 1:10 volume of 3M sodium acetate, pH 5.2 (Quality Biological, Inc.), were added to the RNA solution and vigorously vortexed. 4 volumes of 100% ethanol were added to the mixture and incubated overnight at −20 °C. Subsequently, the RNA samples were centrifuged at 12,000 X G for 30 min at 4 °C and the supernatant was discarded. The RNA pellet was washed with 70% ethanol solution, air-dried at RT for 2 hours and solubilized in 25 μL of RNase free water. The RNA was quantified and checked for protein or TRIzol contamination (measured respectively by A260/280 and A260/230 ratios) using the NanoDrop ND-1000 spectrophotometer.

SIV RNA viral loads in tissue were quantified using the purified RNA (50–1000 ng) by a one-step reverse transcriptase droplet digital PCR (RT-ddPCR) method with ddPCR Supermix for Probes (No dUTP [deoxyuridine triphosphate] Bio-Rad), QX200 Automatic Droplet Generator (Bio-Rad), QX200 Droplet Reader (Bio-Rad), C1000 Touch Thermal Cycler (Bio-Rad), and PX1 PCR Plate Sealer (Bio-Rad) according to the manufacturer's instructions. PCR Reaction conditions were developed according to previously published reaction conditions and SIV gag primer and probe sequences (FAM/BHQ) (20). As internal controls, macaque GAPDH gene primers/probe (VIC/MGB, Applied Biosystems) were used with the following sequences: forward, 5′-CAAGGCTGTGGGCAAGGT-3′; reverse sequence, 5′-GGCCATGCCAGTGAGCTT-3′; probe (VIC-labeled), 5′-ATCCCTGAGCTGAACG −3′. Reactions were set up in duplicate in a 96-well plate. After droplet generation, 40 μL of the reaction was transferred to wells of a 96-well plate. The plates were sealed, and the reactions were carried out in the thermocycler using the following parameters: step 1, 95°C for 10 minutes; step 2, 94°C for 30 seconds and 59°C for 1 minute (step 2 was repeated 39 times for a total of 40 cycles); step 3, 98°C for 10 minutes; and Step 4, 4°C infinite hold. All steps had a ramp rate of 2°C per second. After thermocycling, the reactions were transfer to the QX200 Droplet Reader. The data were analyzed by QuantaSoft Version 1.7 Regulatory Edition. The calculated results from the BioRad reader software were reported as copies/μL. The copy number of RNA in the 20 μL of the ddPCR reaction was converted to RNA copy number per 1000 ng of total RNA.

Sample collection

Approximately 50 weeks post-infection macaques were sacrificed for collection of peripheral blood in EDTA-treated tubes as well as spleen and liver biopsies. Liver biopsies

were collected after 15 minutes of hepatic perfusion with sterile sodium chloride. PBMCs were obtained by centrifugation on Ficoll-Paque PLUS gradients (GE Healthcare, Piscataway, NJ) and red blood cells were lysed with ACK buffer. Spleen biopsies were minced with a scalpel and passed through a 40-μm cell strainer prior to lysis of red blood cells. Liver biopsies were finely minced using surgical scissors and digested in 1 mg/ml of collagenase II (Sigma, St. Louis, MO) on an orbital shaker at 37°C for 30 min. After digestion, liver cells were passed through a sterile gauze strainer and enriched for lymphocytes using a 40% Percoll gradient. All single-cell suspensions (PBMCs, spleen and liver) were washed and re-suspended in R10 medium (RPMI 1640 containing 10% FBS, 2mM L-glutamine, 1% non-essential amino acids, 1% sodium pyruvate and 1X penicillin plus streptomycin). Cells were used fresh for phenotypic characterization of surface NK cell receptors and remaining PBMCs and spleen cells were viably frozen in 90% fetal bovine serum (Invitrogen, Carlsbad, CA) with 10% dimethyl sulfoxide (Sigma-Aldrich) for later use in functional and additional phenotypic assays. Upon thawing, cells were washed and re-suspended in R10 medium at 37°C and 5% CO_2 for 6 h prior to activation.

NK cell stimulation assays

PBMCs and spleen single-cell suspensions were thawed and activated using SIV-specific antibodies, Fc-receptor crosslinking, co-culture with NK-sensitive 721.221 target cells or by NK cell-stimulating cytokines. Cells ($1 – 1.5 \times 10^6$ per well) were stimulated in 200 μl of R10 medium in V-bottom 96-well plates. Cytokine-dependent stimulations were done for 24 h with recombinant macaque IL-15, IL-18 and IL-2 (all from the NIH/NCRR Resource for Nonhuman Primate Immune Reagents, Emory University, Atlanta, GA), and recombinant human IL-12p70 (Peprotech, Rocky Hill, NJ). SIV-specific Fc-mediated activation was performed by culturing cells for 6 h in the presence of 1 μg/ml of native SIV_{mac251} gp120 (Advanced BioScience Laboratories (ABL) Inc., Rockville, MD) and 40 μl (1:5 final dilution) of pooled sera from three SIV-infected rhesus macaques (not part of this study) with high anti-SIV binding titers. Fc-receptor crosslinking and 721.221 cell stimulation were performed for 6 h by adding 4 μl of an APC-Cy7 anti-CD16 antibody (clone 3G8, BD Biosciences, San Jose, CA) or 721.221 cells (5:1 E:T ratio), respectively. In all stimulation conditions, BD GolgiPlug, BD GolgiStop, and BV785 anti-CD107a antibody (clone H4A3, Biolegend, San Diego, CA) were added at the manufacturer's recommended concentrations for the last 5 h of culture. Cells were subsequently washed and expression levels of CD107a and IFN-γ were measured by Flow Cytometry.

Flow Cytometry antibodies

Anti-human fluorochrome-conjugated monoclonal antibodies known to cross-react with rhesus macaque antigens were used, including: APC-Cy7 anti-CD16 (3G8); V450 anti-IFN-γ (B27), anti-CD56 (B159) and anti-CD3 (SP34-2); Alexa Fluor 700 anti-CD3 (SP34-2) and anti-CXCR3 (1C6/CXCR3); PerCP-Cy5.5 anti-CD8 (SK1); PE-Cy7 anti-CD56 (B159); BV650 anti-CD20 (2H7) and anti-CD14 (M5E2); BV711 anti-CD8 (RPA-T8) and anti-CD132 (AG184); PE-Cy5 anti-CD56 (B159); PE-CF594 anti-CD25 (M-A251); and BV786 anti-CD3 (SP34-2), all from BD Biosciences. PerCP-Cy5.5 anti-CD161 (HP-3G1) and APC anti-CD218a (H44) were obtained from eBioscience (San Diego, CA). PE anti-NKG2A (Z199); PC5 anti-NKp30 (Z25); PC7 anti-NKp46 (BAB281) and anti-CD122 (CF1); and

APC anti-NKG2D (ON72) were from Beckman Coulter (Fullerton, CA). QDot605 anti-CD8 (3B5); PE-TexasRed anti-granzyme B (GB11); and the Yellow and Aqua Live/Dead viability dyes were from Invitrogen. FITC anti-perforin (Pf-344) was obtained from MabTech (Cincinnati, OH). BV605 anti-CD279 (EH12.2H7); and BV785 anti-CD107a (H4A3) were obtained from BioLegend. Alexa Fluor 700 anti-CD212 (69310) was purchased from R&D Systems (Minneapolis, MN). FITC anti-FcεRI (rabbit polyclonal, FCABS400F) was obtained from EMD Millipore (Billerica, MA). Purified rabbit anti-human CD57 polyclonal antibody (LS-C180182) was purchased from LS Bio (Seattle, WA) and detected using DyLight649-conjugated donkey anti-rabbit IgG antibody from BioLegend. QDot655 anti-CD4 (19Thy-5D7) was obtained from the NIH Nonhuman Primate Reagent Resource (Boston, MA). Cells were stained for specific surface molecules, fixed and permeabilized with a Cytofix/Cytoperm Kit (BD Biosciences), and then stained for specific intracellular molecules. At least 250,000 singlet events (PBMCs) were acquired on a LSR II (BD Biosciences) and analyzed using FlowJo Software (Treestar Inc., Ashland, OR). For all samples, gating was established using a combination of isotype and fluorescence-minus-one controls.

Statistical analysis

Data were analyzed as described in figure legends using Prism (v6.01, GraphPad Software). A p value ≤ 0.05 was considered statistically significant.

RESULTS

Immunological and virological characteristics of samples used in this study

SIV_{mac251}-infected rhesus macaques were categorized as controlling or non-controlling based on their chronic viral load levels (Fig. 1A–B). SIV controlling and non-controlling macaques required the same number of low-dose repetitive SIV_{mac251} challenges in order to become infected (Fig. 1C). As expected, post-infection peak (Fig. 1D) and necropsy (Fig. 1E) viral loads were significantly higher in SIV non-controlling macaques when compared to controlling macaques in plasma, as well as in cells from the spleen and PBMCs. Both SIV controlling and non-controlling macaques were necropsied at similar post-infection time points (Fig. 1F). Initially, we immunophenotyped total NK cells ($CD20^{-}CD14^{-}CD3^{-}CD8^{+}NKG2A^{+}$) in single-cell suspensions from PBMCs, spleen and liver at the time of necropsy (Supp. Fig. 1). As shown in Fig. 2A, no differences in the proportion of total NK cells in PBMCs and liver were observed between uninfected (naïve) and SIV-infected controlling (low VL) and non-controlling (high VL) rhesus macaques. On the other hand, high VL macaques had significantly fewer NK cells in the spleen when compared to naïve and low VL macaques (Fig. 2A). When evaluating the CD16- and CD56-based subset distribution of NK cells we observed no significant changes in the proportion of $CD56^{+}$ NK cells in the PBMCs and liver and a significant increase in the abundance of $CD56^{+}$ NK cells in the spleen of high VL macaques when compared to low VL macaques (Fig. 2B). Similarly, while no differences were observed in the abundance of $CD16^{+}$ NK cells in the PBMCs, a significant increase in their proportion was observed in the spleen and liver cells in both groups of SIV-infected macaques when compared to naïve animals (Fig. 2C). In contrast, $CD56^{-}CD16^{-}$ (double negative, DN) NK cells were significantly decreased

in the spleen and liver of high VL macaques when compared to naïve animals (Fig. 2D). Interestingly, when evaluating SIV-infected animals as a single group, a positive correlation between the abundance of splenic $CD56^+$ NK cells and the plasma viral load at necropsy was seen (Fig. 2E). On the other hand, an inverse correlation between the percentages of hepatic DN NK cells and the necropsy plasma viral load was observed (Fig. 2F).

Expression of CXCR3 and NKG2D correlate with decreased chronic viral loads in SIV controlling macaques

Given that NK cell functional activity is tightly controlled by a balance of inhibitory and activatory signals (6), and that NK cell migratory potential is controlled by the expression of diverse chemokine surface receptors (23), we evaluated the expression of several cytotoxic and migratory markers on NK cells from high and low VL SIV-infected macaques. Using anti-human clones of fluorochrome-conjugated monoclonal antibodies cross-reactive with rhesus macaque cells we first examined the expression levels of NKp30, NKp46, CXCR3, and NKG2D. Interestingly, while no variation in the abundance of $NKp30^+NKp46^+$ NK cells was observed in the PBMCs of naïve and SIV-infected macaques, significantly decreased expression of these cells was observed in splenic NK cells of low VL macaques when compared to naïve animals (Fig. 3A). At the same time an increased abundance of $NKp30^+NKp46^+$ NK cells was observed in liver samples from high VL macaques. A correlation analysis using all SIV-infected animals displayed a significant positive correlation between the abundance of $NKp30^+NKp46^+$ NK cells and the necropsy plasma viral load both in PBMCs and spleen cells (Fig. 3B). Although CXCR3 expression by NK cells in the PBMCs and spleen of naïve and SIV-infected animals was comparable, a significant decrease in $CXCR3^+$ NK cells was observed in the liver of high VL macaques (Fig. 3C). Furthermore, CXCR3 expression in liver NK cells of low VL macaques correlated inversely with the necropsy plasma viral load (Fig. 3D). We observed no significant differences in the expression of NKG2D by NK cells in PBMCs, spleen or liver (Fig. 3E). Despite this, a significant inverse correlation was observed between the expression of NKG2D in circulatory NK cells and the plasma viral loads at necropsy in low VL animals (Fig. 3F).

Other cytotoxic and functional NK cell markers evaluated in the present study included CD161, PD-1, perforin and granzyme B. While CD161 expression was comparable in PBMC and spleen NK cells of naïve and SIV-infected macaques, its expression was significantly decreased in liver NK cells of high VL macaques (Fig. 4A). A significant increase in PD-1 expression by NK cells was only observed in the liver of low VL macaques (Fig. 4B). Similarly, significant increases in perforin (Fig. 4C) and granzyme B (Fig. 4D) expression were observed in spleen and liver NK cells of low VL macaques, while perforin was also increased in splenic NK cells of high VL macaques compared to naïve animals.

Given the recent evidence that NK cells can develop long-term memory-like functional responses (10, 24–26), and that these antigen-specific NK cell responses in humans are associated with expression of CD57 and the lack of the intracellular adaptor protein, FcεRIγ (27–30), we evaluated CD57 and FcεRIγ expression in circulatory and splenic NK cells. Similar to humans, FcεRIγ-deficient NK cells in rhesus macaques were detectable at

variable rates (Fig. 5A). FcεRIγ-deficient NK cell frequencies ranged from 4% to 70% in blood, and 4% to 82% in spleen. Determination of FcεRIγ-deficient and $CD57^+$ NK cells was not performed in liver cells due to a lack of viably frozen samples. While no statistically significant differences were observed between naïve and SIV-infected macaques, a marginally non-significant (p=0.05) increase in FcεRIγ-deficient NK cells was observed in the spleen of low VL SIV-infected macaques (Fig. 5B). Unlike their human counterparts, $CD57^+$ NK cells were detected in relative high abundance in the blood and spleen of naïve and SIV-infected rhesus macaques (Fig. 5C). Despite this, only a marginally non-significant (p=0.06) decrease in the abundance of circulatory $CD57^+$ NK cells was observed in high VL macaques when compared to naïve animals (Fig. 5D).

Increased NK cell responsiveness to IL-15 and IL-18 is associated with lower chronic viremia in SIV-controlling macaques

Given that HIV/SIV infection alters the NK cell surface receptor repertoire and impairs the capacity of these cells to respond to and produce cytokines (31), we evaluated the responsiveness of NK cells from high and low VL SIV-infected rhesus macaques to exogenous cytokine stimulation. Due to limitation of liver NK cells, only PBMC and splenic NK cells were evaluated. PBMCs were directly activated with IL-15 (50 ng/ml), IL-18 (500 ng/ml), IL-12 (500 ng/ml), IL-2 (500 ng/ml) and a combination of IL-18+IL-12+IL-2 (500 ng/ml each). When measuring NK cell activation based on the production of IFN-γ (Fig. 6A), stimulation of PBMCs from naïve macaques always led to higher levels of cytokine production when compared to SIV-infected macaques. As shown in Figure 6A, statistically significant differences were observed between naïve and low VL macaques when stimulated with IL-15 (p<0.01) and IL-2 (p<0.05). Interestingly, when correlating the capacity of circulatory NK cells to respond to different cytokine stimuli, production of IFN-γ in response to IL-15 (Fig. 6B) and IL-18 (Fig. 6C) stimulation was directly correlated with the number of SIV_{mac251} intrarectal challenges needed for infection. These correlations were only observed in low VL macaques. Moreover, when stimulating splenocytes in similar conditions, we observed a statistically significant decrease in the production of IFN-γ in response to IL-15 stimulation in low VL macaques when compared to naïve animals (Fig. 6D). Furthermore, statistically significant decreases in NK cell activation were also observed between naïve and high VL macaques after stimulation with IL-12, IL-2 and IL-18+IL-2+IL-12 (Fig. 6D).

Having observed that SIV infection leads to a decreased responsiveness to exogenous cytokine stimulation, we next investigated if SIV-infected macaques exhibited differences in expression levels of surface cytokine receptors. After screening several anti-human cytokine receptor monoclonal antibodies against rhesus macaque cells we identified 5 cross-reactive clones (CD25/IL-2Rα, CD122/IL-2Rβ, CD132/IL-2Rγ, CD218a/IL-18Rα and IL-12$Rβ_1$). While no significant differences were observed in the surface expression levels of CD218a in PBMCs or spleen in SIV-infected macaques (Fig. 7A), significant inverse correlations were observed between the expression of CD218a in PBMCs (Fig. 7B) and spleen (Fig. 7C) and peak plasma viral load. Similarly, a significant positive correlation was observed between CD218a expression in PBMCs and the number of SIV_{mac251} challenges required for infection (Fig. 7D). Importantly, these three correlations were only observed in low VL

macaques. The fact that the peak viral load was inversely correlated with the number of challenges in the low VL macaques (Fig. 7E) provides a possible explanation for the NK cell correlations at necropsy with the number of challenges needed for infection. Macaques requiring more viral exposures exhibited partial protection as they developed lower viral loads, which likely were sustained into the chronic phase of infection. Finally, we did not observe any difference in the expression levels of CD25, CD132, or IL-12Rβ1 in any of the assayed PBMC or spleen samples (Supp. Fig. 2A–C). Despite this, we did observe a significant decrease in CD122 expression by NK cells in PBMCs of both low and high VL macaques when compared to naïve macaques (Supp. Fig. 2D).

Increased cytotoxic and Ab-dependent NK cell function are associated with lower viremia and delayed SIV acquisition in SIV controlling macaques

After observing that SIV-infection leads to an alteration in NK cell natural cytotoxicity receptor (NCR) expression, as well as to impairment in the capacity to respond to exogenous cytokine stimulation, we evaluated NK cells for their Ab-dependent functionality. NK cells are capable of mediating antigen-specific immune responses by interacting with pathogen-specific antibodies through surface Fc receptors (32). Importantly, the capacity of circulatory and tissue-resident NK cells to mediate Ab-dependent Fc-mediated responses has been shown to be one of the factors contributing to the limited success of the RV144 vaccine trial (33, 34). Initially, we evaluated the capacity of circulatory and splenic NK cells to become activated after direct crosslinking of surface CD16 using a fluorochrome conjugated anti-CD16 antibody (35). As shown in Figure 8A, we observed a significantly decreased capacity of circulatory NK cells of SIV-infected macaques to degranulate ($CD107a^+$) or to produce IFN- γ in response to CD16 crosslinking when compared to naïve macaques. On the other hand, no significant differences were observed between naïve and SIV-infected macaques when splenic NK cells were activated through direct CD16 crosslinking (Fig. 8A, Spleen). Given that CD16 crosslinking is a surrogate marker of Fc-mediated function, we next tested the capacity of NK cells to become activated directly by SIV-specific antibodies in the presence of gp120 protein (17, 36, 37). Similar to what we observed by crosslinking CD16, NK cells within the PBMCs of SIV-infected macaques displayed a decreased capacity to respond to activation (both as CD107a expression and IFN- γ production) by the pool of high titer SIV-specific antibodies (Fig. 8B, PBMCs). Decreased SIV-specific antibody responses by splenic NK cells were only observed in high VL, but not low VL, SIV-infected macaques (Fig. 8B, Spleen). Interestingly, in all SIV-infected macaques, a negative correlation was observed between the capacity of splenic NK cells to become activated ($CD107a^+$) in response to SIV-specific antibodies and the plasma viral load at necropsy (Fig. 8D).

Finally, as NK cells can also mediate direct cytotoxic function against virus-infected cells, we evaluated the response of circulatory and splenic NK cells when co-cultured with MHC-I-devoid 721.221 target cells. While circulatory NK cell activation in response to 721.221 cell co-culture was comparable between naïve and low VL macaques, high VL macaques displayed significantly lower levels of activation (Fig. 8C, PBMCs). A similar trend was observed for $CD107a^+$ NK cells in the spleen (Fig. 8C, Spleen) along with a significant decrease in IFN-γ expression. Notably, when evaluating all SIV infected macaques in a

single group, we observed a direct correlation between the natural cytotoxic response of circulatory NK cells (both for CD107a upregulation and IFN- γ production) and the number of SIV_{mac251} challenges needed for infection (Fig. 8E). Collectively, our data indicate that a number of phenotypic differences and functional NK cell responses detected in the circulation and in tissue-resident NK cells are related to the maintenance of low viral loads in SIV controlling rhesus macaques.

DISCUSSION

In the present study we investigated the phenotype and functional responses of NK cells present in the circulation and tissues of SIV controlling macaques. Specifically, we evaluated the capacity of NK cells to respond to cytokine stimulation, express distinct cytokine receptors and perform Ab-dependent and –independent cytotoxic function.

Initially we examined expression of CD56 and CD16 by circulatory and tissue-resident NK cells. While NK cells in peripheral blood of naïve, Low VL and High VL macaques exhibited no differences in sub-populations defined by these markers, some significant differences were seen in tissue-resident NK cells with a decline in the total proportion of NK cells in the High VL group along with an increase in splenic NK $CD56^+$ cells and a general increase in $CD16^+$ NK cells of the spleen and liver in SIV-infected animals (Fig. 2A–C). Of greater interest, however, was the significant decline in DN NK cells of both spleen and liver in the High VL macaques (Fig. 2D). The DN NK cells were inversely correlated with plasma viral loads at the time of necropsy (Fig. 2F), suggesting that this subpopulation might influence viremia control. This observation warrants additional investigation, but it is noteworthy that human DN NK cells have been reported to have the capacity for potent cytotoxic activity and IFN-γ production (38).

With regard to additional phenotypic markers, no significant changes among the three groups of macaques were detected in circulatory NK cells, although the frequency of NK cells in PBMC expressing the activatory receptors NKp30 and NKp46 was directly correlated with viral loads at the time of necropsy (Fig. 3B) and NKG2D-expressing NK cells in PBMC were inversely correlated with viremia in the Low VL macaques (Fig. 3F). The latter observation may relate to the complementary role of NKG2D with NCRs, where the triggering of NK cells may depend on the action of both together (39). Additional differences were observed among the tissue-resident NK cells, most notably enhanced frequencies of perforin and granzyme B expressing NK cells in the spleen and liver of Low VL macaques (Fig. 4C, D). Nevertheless, these cells were not associated with viremia control in our analyses.

Recent studies have identified a subset of murine NK cells that have the capacity to establish immunologic memory and respond to secondary stimulation (40, 41). Antigen-specific NK memory has also been observed in rhesus macaques (9). Further, a subset of NKG2C/CD57 positive and FcRγ deficient human NK cells has been linked to antigen-specific responses to cytomegalovirus reactivation (27, 29). Interestingly, expansion of these memory-like NK cells seems to be driven in an antibody-dependent manner (27). We were particularly interested in identifying a potential role for FcεRIγ deficiency (28) or CD57 expression (29)

as markers of rhesus macaque memory-like NK cells that might contribute to control of viremia in the chronic phase. Interestingly, FcεRIγ-deficient rhesus NK cells were present at abundances similar to those reported for circulatory human NK cells (Fig. 5B). When looking at splenic NK cells we only observed a marginally non-significant increase in the abundance of FcεRIγ-deficient NK cells in Low VL macaques (Fig. 5B). Interestingly however, low VL macaques also displayed a higher capacity to mediate SIV-specific Ab-dependent function (Fig. 8B), which is a hallmark of FcεRIγ-deficient NK cells (27). This activity was inversely correlated with plasma viral loads at necropsy (Fig. 8D). CD57, a second phenotypic marker of memory-like NK cells was also detected on rhesus macaque NK cells (Fig. 5C–D), but was more abundantly expressed compared to what has been reported for humans (42). Given the cytomegalovirus (CMV)-specificity of human $CD57^+$ NK cells, the higher overall expression of CD57 in rhesus NK cells might be partially explained by the higher overall incidence of CMV in the rhesus population (up to 90% in captive rhesus macaques) (43). In fact, in the animals tested here, all but one (R252 in the high VL group) was CMV sero-positive (data not shown), which further supports the increased abundance of $CD57^+$ NK cells. Given the limited number of SIV controlling macaques used in this study, further experiments with larger animal cohorts are required to define the role of FcεRIγ-deficient NK cells in mediating control of chronic SIV viremia.

NK cells of SIV infected macaques, both Low VL and High VL groups were clearly dysfunctional. They responded poorly to cytokine stimulation (Fig. 6), which was not due to lack of cytokine receptor expression (Fig. 7, Supplemental Fig. 2). Further functional responses, including response to CD16 cross-linking, antibody-dependent Fc-mediated responses, and natural cytotoxicity responses, were impaired (Fig. 8). Importantly, this functional impairment affects NK cells in two distinct anatomical locations (circulation and spleen), which are known to be phenotypically and functionally distinct based on their expression patterns for CD16 and CD56 (Fig. 2) and (5). Nevertheless, the correlations of various NK cell subpopulations of SIV-infected or Low VL macaques with viremia control, including DN, CXCR3, NKG2D, and IL-18Rα, along with functional NK mediated antibody-dependent responses, suggest that NK cells have a clear and persistent influence on disease outcome.

Overall, our study illustrates the polyfunctional capacity of NK cells which exert both Ab-dependent and Ab-independent cytotoxic function. Moreover, certain NK cell subsets expressing unique phenotypic markers (CXCR3 and NKG2D) were enriched in animals displaying lower viral loads. NK antigen-specific memory cells have now been identified in both humans and non-human primates. Given the inverse correlations of chronic viremia with several phenotypic and functional NK characteristics, aiming to induce certain NK cell populations through vaccination may potentially augment the protective efficacy of HIV/SIV vaccines.

Supplementary Material

Refer to Web version on PubMed Central for supplementary material.

Acknowledgments

We gratefully acknowledge the animal caretakers at the NCI Animal Facility for expert animal care. We thank Thorsten Demberg, Olivia Ying, Leia Miller-Novak and Thomas Musich for assistance with sample processing. We thank Katherine McKinnon and Sophia Brown (Vaccine Branch Flow Core, NCI) for expert advice in Flow Cytometry; the NIH/NCRR Resource for Nonhuman Primate Immune Reagents (Emory University, Atlanta, GA) for the macaque recombinant proteins; and Dr. Bernard A.P. Lafont (Laboratory of Molecular Microbiology, NIAID) for providing the 721.221 cells. The following reagent was obtained through the NIH Nonhuman Primate Reagent Resource: QDot655 anti-CD4 antibody.

This research was supported by the Intramural Research Program of the National Institutes of Health, National Cancer Institute.

References

1. Vivier E, Raulet DH, Moretta A, Caligiuri MA, Zitvogel L, Lanier LL, Yokoyama WM, Ugolini S. Innate or adaptive immunity? The example of natural killer cells. Science. 2011; 331:44–49. [PubMed: 21212348]
2. Cooper MA, Fehniger TA, Caligiuri MA. The biology of human natural killer-cell subsets. Trends Immunol. 2001; 22:633–640. [PubMed: 11698225]
3. Webster RL, Johnson RP. Delineation of multiple subpopulations of natural killer cells in rhesus macaques. Immunology. 2005; 115:206–214. [PubMed: 15885126]
4. Vargas-Inchaustegui DA, Demberg T, Robert-Guroff M. A CD8alpha(−) subpopulation of macaque circulatory natural killer cells can mediate both antibody-dependent and antibody-independent cytotoxic activities. Immunology. 2011; 134:326–340. [PubMed: 21978002]
5. Reeves RK, Gillis J, Wong FE, Yu Y, Connole M, Johnson RP. CD16- natural killer cells: enrichment in mucosal and secondary lymphoid tissues and altered function during chronic SIV infection. Blood. 2010; 115:4439–4446. [PubMed: 20339088]
6. Mavilio D, Benjamin J, Daucher M, Lombardo G, Kottilil S, Planta MA, Marcenaro E, Bottino C, Moretta L, Moretta A, Fauci AS. Natural killer cells in HIV-1 infection: dichotomous effects of viremia on inhibitory and activating receptors and their functional correlates. Proc Natl Acad Sci U S A. 2003; 100:15011–15016. [PubMed: 14645713]
7. Ortaldo JR, Herberman RB. Heterogeneity of natural killer cells. Annu Rev Immunol. 1984; 2:359–394. [PubMed: 6399848]
8. Mandal A, Viswanathan C. Natural killer cells: In health and disease. Hematol Oncol Stem Cell Ther. 2015; 8:47–55. [PubMed: 25571788]
9. Reeves RK, Li H, Jost S, Blass E, Li H, Schafer JL, Varner V, Manickam C, Eslamizar L, Altfeld M, von Andrian UH, Barouch DH. Antigen-specific NK cell memory in rhesus macaques. Nat Immunol. 2015; 16:927–932. [PubMed: 26193080]
10. Min-Oo G, Kamimura Y, Hendricks DW, Nabekura T, Lanier LL. Natural killer cells: walking three paths down memory lane. Trends Immunol.
11. Sun JC, Lanier LL. Versatility in NK cell memory. Immunol Cell Biol. 89:327–329.
12. Rydyznski CE, Waggoner SN. Boosting vaccine efficacy the natural (killer) way. Trends Immunol. 2015; 36:536–546. [PubMed: 26272882]
13. Borrow P. Innate immunity in acute HIV-1 infection. Curr Opin HIV AIDS. 2011; 6:353–363. [PubMed: 21734567]
14. Tomescu C, Abdulhaqq S, Montaner LJ. Evidence for the innate immune response as a correlate of protection in human immunodeficiency virus (HIV)-1 highly exposed seronegative subjects (HESN). Clin Exp Immunol. 164:158–169.
15. Ackerman ME, Mikhailova A, Brown EP, Dowell KG, Walker BD, Bailey-Kellogg C, Suscovich TJ, Alter G. Polyfunctional HIV-Specific Antibody Responses Are Associated with Spontaneous HIV Control. PLoS Pathog. 2016; 12:e1005315. [PubMed: 26745376]
16. Isitman G, Lisovsky I, Tremblay-McLean A, Kovacs C, Harris M, Routy JP, Bruneau J, Wainberg MA, Tremblay C, Bernard NF. Antibody-Dependent Cellular Cytotoxicity Activity of Effector

Cells from HIV-Infected Elite and Viral Controllers. AIDS Res Hum Retroviruses. 2016; 32:1079–1088. [PubMed: 27499379]

17. Thobakgale CF, Fadda L, Lane K, Toth I, Pereyra F, Bazner S, Ndung'u T, Walker BD, Rosenberg ES, Alter G, Carrington M, Allen TM, Altfeld M. Frequent and strong antibody-mediated natural killer cell activation in response to HIV-1 Env in individuals with chronic HIV-1 infection. J Virol. 2012; 86:6986–6993. [PubMed: 22496218]
18. Vargas-Inchaustegui DA, Xiao P, Tuero I, Patterson LJ, Robert-Guroff M. NK and CD4+ T cell cooperative immune responses correlate with control of disease in a macaque simian immunodeficiency virus infection model. J Immunol. 2012; 189:1878–1885. [PubMed: 22798665]
19. Tuero I, Mohanram V, Musich T, Miller L, Vargas-Inchaustegui DA, Demberg T, Venzon D, Kalisz I, Kalyanaraman VS, Pal R, Ferrari MG, LaBranche C, Montefiori DC, Rao M, Vaccari M, Franchini G, Barnett SW, Robert-Guroff M. Mucosal B Cells Are Associated with Delayed SIV Acquisition in Vaccinated Female but Not Male Rhesus Macaques Following SIVmac251 Rectal Challenge. PLoS Pathog. 2015; 11:e1005101. [PubMed: 26267144]
20. Lee EM, Chung H-K, Livesay J, Suschak J, Finke L, Hudacik L, Galmin L, Bowen B, Markham P, Cristillo A, Pal R. Molecular methods for evaluation of virological status of nonhuman primates challenged with simian immunodeficiency or simian-human immunodeficiency viruses. J Virol Methods. 2010; 163:287–294. [PubMed: 19878696]
21. Romano JW, Shurtliff RN, Dobratz E, Gibson A, Hickman K, Markham PD, Pal R. Quantitative evaluation of simian immunodeficiency virus infection using NASBA technology. J Virol Methods. 2000; 86:61–70. [PubMed: 10713377]
22. Joseph Sambrook, J., Russell, DW. Molecular Cloning. 3. Vol. 3. Cold Spring Harbor Laboratory Press; Cold Spring Harbor, NY: 2001.
23. Robertson MJ. Role of chemokines in the biology of natural killer cells. J Leukoc Biol. 2002; 71:173–183. [PubMed: 11818437]
24. Cooper MA, Elliott JM, Keyel PA, Yang L, Carrero JA, Yokoyama WM. Cytokine-induced memory-like natural killer cells. Proc Natl Acad Sci U S A. 2009; 106:1915–1919. [PubMed: 19181844]
25. Cooper MA, Yokoyama WM. Memory-like responses of natural killer cells. Immunol Rev. 2010; 235:297–305. [PubMed: 20536571]
26. Horowitz A, Behrens RH, Okell L, Fooks AR, Riley EM. NK cells as effectors of acquired immune responses: effector CD4+ T cell-dependent activation of NK cells following vaccination. J Immunol. 2010; 185:2808–2818. [PubMed: 20679529]
27. Lee J, Zhang T, Hwang I, Kim A, Nitschke L, Kim M, Scott JM, Kamimura Y, Lanier LL, Kim S. Epigenetic modification and antibody-dependent expansion of memory-like NK cells in human cytomegalovirus-infected individuals. Immunity. 2015; 42:431–442. [PubMed: 25786175]
28. Hwang I, Zhang T, Scott JM, Kim AR, Lee T, Kakarla T, Kim A, Sunwoo JB, Kim S. Identification of human NK cells that are deficient for signaling adaptor FcRgamma and specialized for antibody-dependent immune functions. Int Immunol. 2012; 24:793–802. [PubMed: 22962434]
29. Hendricks DW, Balfour HH Jr, Dunmire SK, Schmeling DO, Hogquist KA, Lanier LL. Cutting edge: NKG2C(hi)CD57+ NK cells respond specifically to acute infection with cytomegalovirus and not Epstein-Barr virus. J Immunol. 2014; 192:4492–4496. [PubMed: 24740502]
30. Gooneratne SL, Center RJ, Kent SJ, Parsons MS. Functional advantage of educated KIR2DL1(+) natural killer cells for anti-HIV-1 antibody-dependent activation. Clin Exp Immunol. 2016; 184:101–109. [PubMed: 26647083]
31. Ansari AW, Ahmad F, Meyer-Olson D, Kamarulzaman A, Jacobs R, Schmidt RE. Natural killer cell heterogeneity: cellular dysfunction and significance in HIV-1 immuno-pathogenesis. Cell Mol Life Sci. 2015; 72:3037–3049. [PubMed: 25939268]
32. Wang W, Erbe AK, Hank JA, Morris ZS, Sondel PM. NK Cell-Mediated Antibody-Dependent Cellular Cytotoxicity in Cancer Immunotherapy. Front Immunol. 2015; 6:368. [PubMed: 26284063]
33. Vargas-Inchaustegui DA, Robert-Guroff M. Fc Receptor-Mediated Immune Responses: New Tools but Increased Complexity in HIV Prevention. Curr HIV Res. 2013; 11:407–420. [PubMed: 24191937]

34. Kim JH, Excler JL, Michael NL. Lessons from the RV144 Thai phase III HIV-1 vaccine trial and the search for correlates of protection. Annu Rev Med. 2015; 66:423–437. [PubMed: 25341006]

35. Parsons MS, Tang CC, Jegaskanda S, Center RJ, Brooks AG, Stratov I, Kent SJ. Anti-HIV antibody-dependent activation of NK cells impairs NKp46 expression. J Immunol. 2014; 192:308–315. [PubMed: 24319263]

36. Chung AW, Rollman E, Center RJ, Kent SJ, Stratov I. Rapid degranulation of NK cells following activation by HIV-specific antibodies. J Immunol. 2009; 182:1202–1210. [PubMed: 19124764]

37. Stratov I, Chung A, Kent SJ. Robust NK cell-mediated human immunodeficiency virus (HIV)-specific antibody-dependent responses in HIV-infected subjects. J Virol. 2008; 82:5450–5459. [PubMed: 18353957]

38. Stabile H, Nisti P, Morrone S, Pagliara D, Bertaina A, Locatelli F, Santoni A, Gismondi A. Multifunctional human CD56 low CD16 low natural killer cells are the prominent subset in bone marrow of both healthy pediatric donors and leukemic patients. Haematologica. 2015; 100:489–498. [PubMed: 25596273]

39. Moretta A, Bottino C, Vitale M, Pende D, Cantoni C, Mingari MC, Biassoni R, Moretta L. Activating receptors and coreceptors involved in human natural killer cell-mediated cytolysis. Annu Rev Immunol. 2001; 19:197–223. [PubMed: 11244035]

40. Paust S, Gill HS, Wang BZ, Flynn MP, Moseman EA, Senman B, Szczepanik M, Telenti A, Askenase PW, Compans RW, von Andrian UH. Critical role for the chemokine receptor CXCR6 in NK cell-mediated antigen-specific memory of haptens and viruses. Nat Immunol. 2010; 11:1127–1135. [PubMed: 20972432]

41. Sun JC, Beilke JN, Lanier LL. Adaptive immune features of natural killer cells. Nature. 2009; 457:557–561. [PubMed: 19136945]

42. Lopez-Verges S, Milush JM, Schwartz BS, Pando MJ, Jarjoura J, York VA, Houchins JP, Miller S, Kang SM, Norris PJ, Nixon DF, Lanier LL. Expansion of a unique CD57(+)NKG2Chi natural killer cell subset during acute human cytomegalovirus infection. Proc Natl Acad Sci U S A. 2011; 108:14725–14732. [PubMed: 21825173]

43. Hansen SG, Strelow LI, Franchi DC, Anders DG, Wong SW. Complete sequence and genomic analysis of rhesus cytomegalovirus. J Virol. 2003; 77:6620–6636. [PubMed: 12767982]

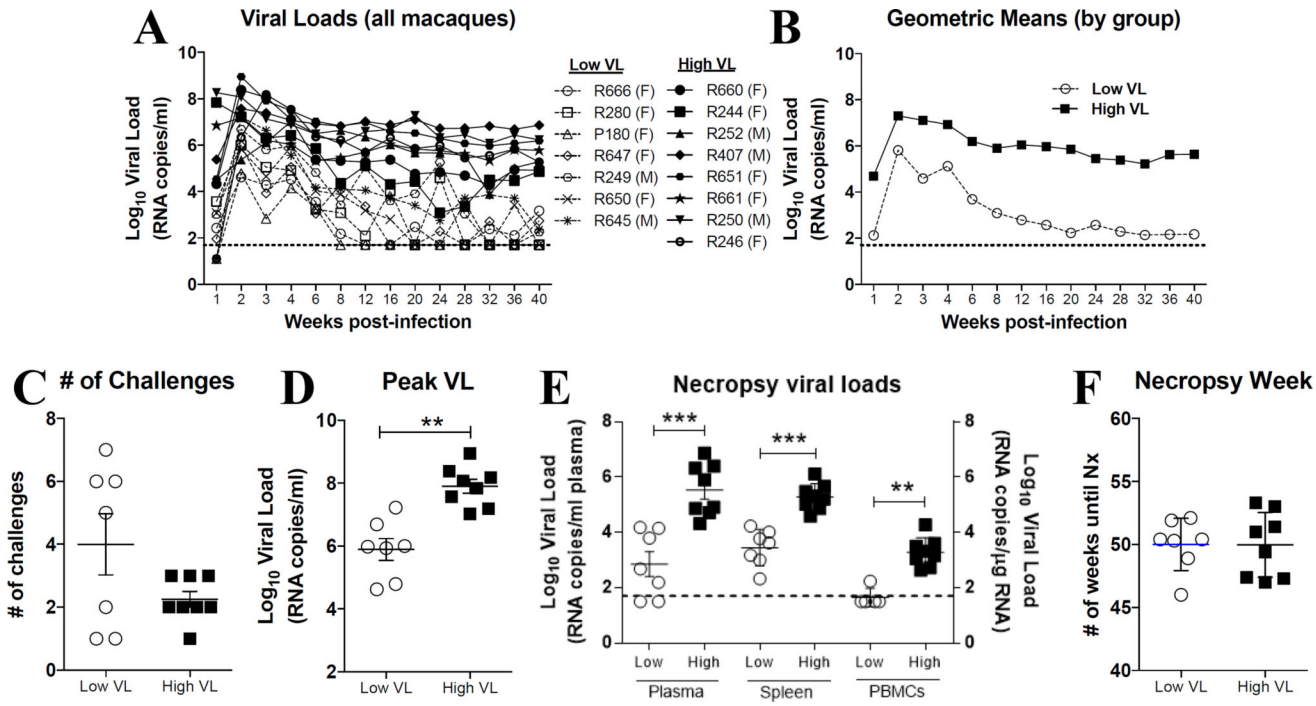

Fig. 1. Virological characteristics of macaques used in the present study

SIV-infected rhesus macaques used in this study were part of a previously reported vaccination study (19). Macaques were divided into two groups based on their chronic plasma viral loads, as previously described (18). (A–B) High viral load macaques (High VL, solid lines) displayed plasma viral loads ≥ 10^4 RNA copies per ml of plasma. Low viral load macaques (Low VL, dashed lines) had plasma viral loads ≤ 10^4 RNA copies per ml of plasma. Plasma viral loads for all macaques are displayed for a 40-week post-infection period for individual animals (A) or as geometric means by group (B). (C–F) Low and high viral load macaques were also evaluated for: number of challenges required for infection (C), peak viral load (D), viral load at necropsy in plasma, spleen and PBMCs (E) and week at which necropsy samples were collected (F). Data reported are means ± SEM. **, $p<0.01$ and ***, $p<0.001$ indicate statistically significant differences by Mann-Whitney *t* test.

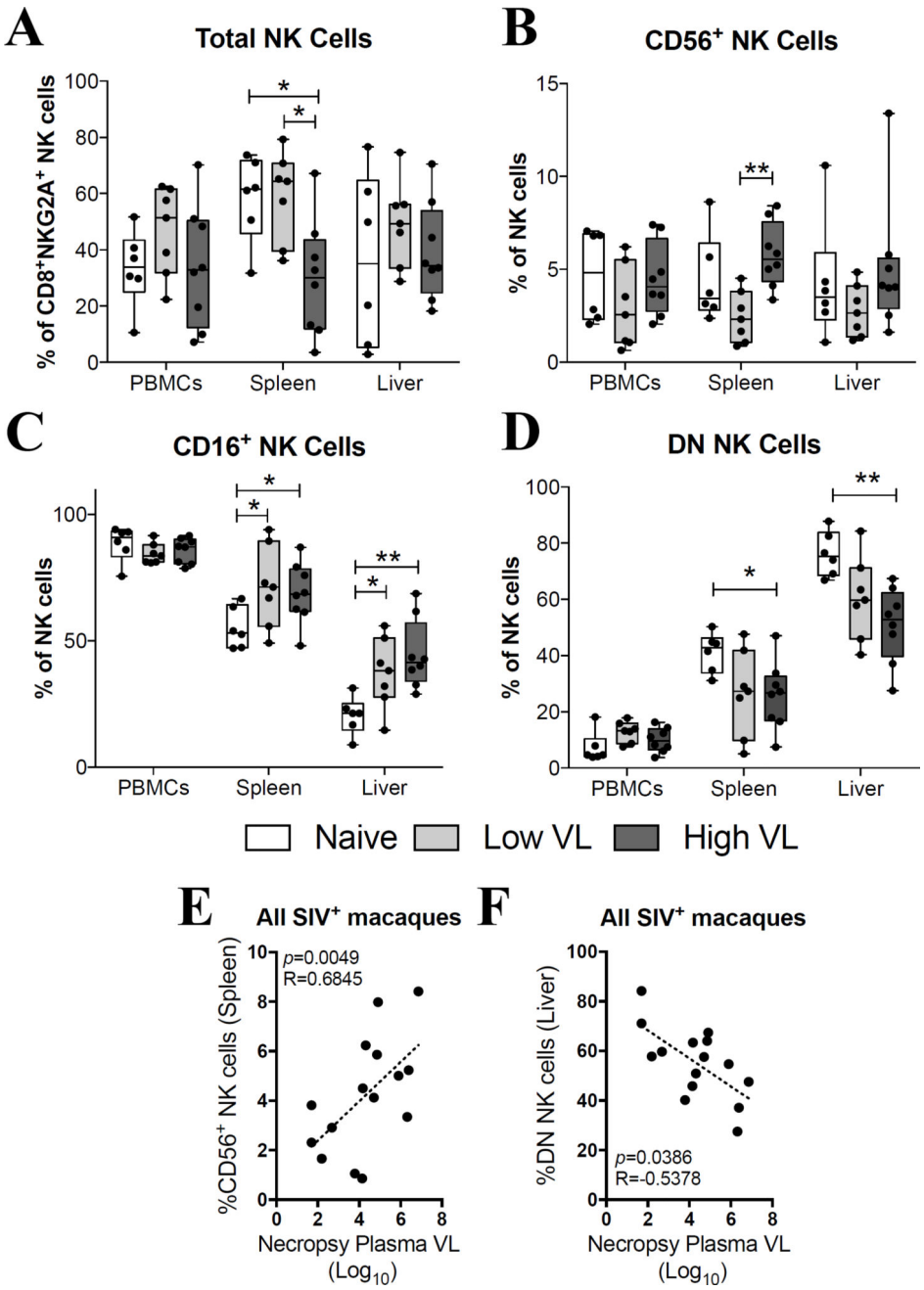

Fig. 2. Phenotypic characterization of circulatory and tissue-resident NK cells at the time of necropsy

Lymphocyte single-cell suspensions were purified from blood, spleen and liver of SIV-negative (naïve) and SIV-infected (Low VL and High VL) macaques and stained fresh for flow cytometric analysis. (A–D) Total rhesus macaque NK cells were defined as $CD20^{-}CD14^{-}CD3^{-}CD8^{+}NKG2A^{+}$ cells (A) and further divided into $CD56^{+}$ (B), $CD16^{+}$ (C) and $CD56^{-}CD16^{-}$ double negative (D) NK cells based on their cell surface expression levels of CD16 and CD56. Data are shown as minimum to maximum floating bars with a horizontal line representing the mean. *, $p<0.05$ and **, $p<0.01$ indicate statistically significant differences by Mann-Whitney *t* test. (E–F) Correlations between plasma viral

loads at necropsy and abundance of spleen $CD56^{+}$ (E) and liver DN (F) NK cells. Spearman's correlation analysis was used to determine statistical significance in E and F.

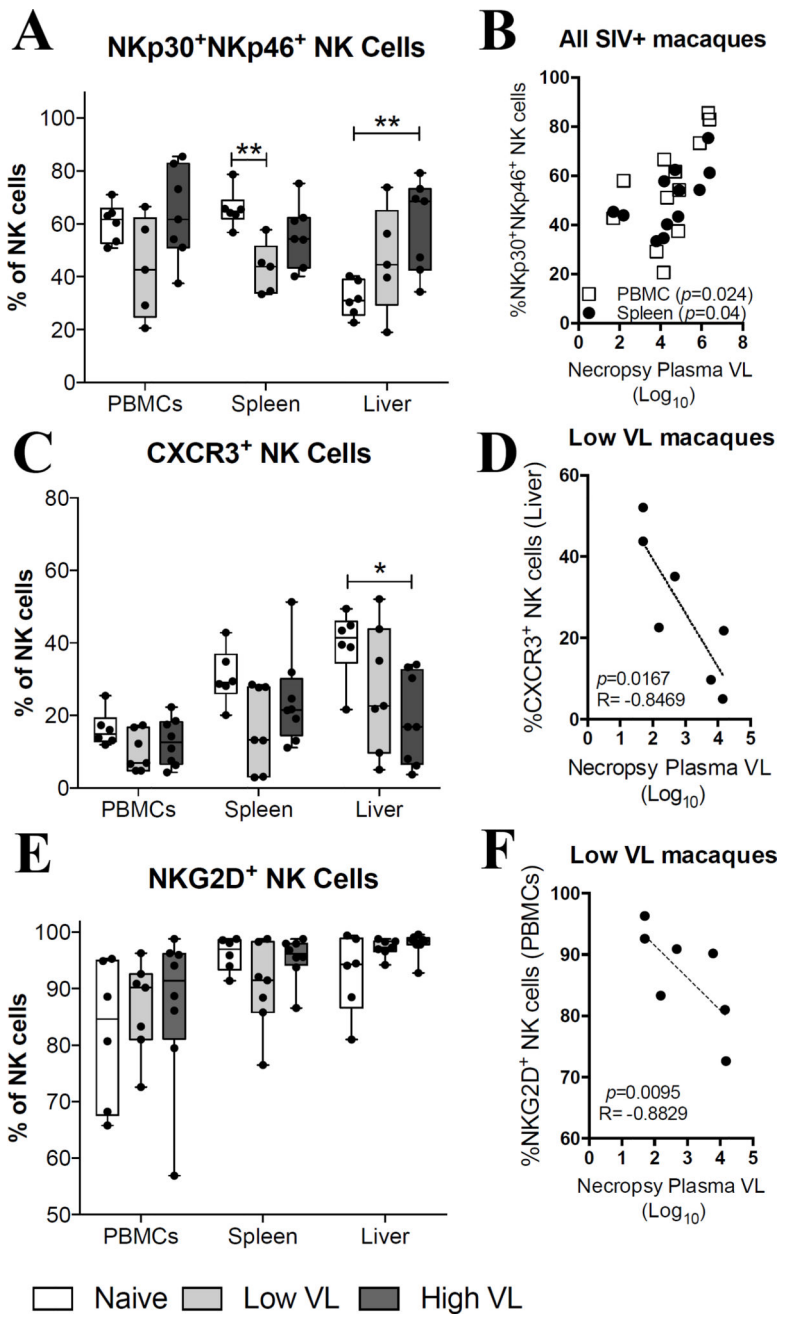

Fig. 3. NK cell expression of CXCR3 and NKG2D correlates with decreased chronic viral loads in SIV controlling macaques

Lymphocyte single-cell suspensions were purified from blood, spleen and liver of SIV-negative (naïve) and SIV-infected (Low VL and High VL) macaques and stained fresh for flow cytometric analysis. (A–F) Expression of NKp30 and NKp46 (A), CXCR3 (C) and NKG2D (E) by circulatory and tissue resident NK cells from naïve, low VL and high VL rhesus macaques. Correlations between plasma viral loads at necropsy and splenic and circulatory $NKp30^{+}NKp46^{+}$ NK cells in all SIV-infected macaques (B), liver-resident CXCR3+ NK cells of low VL macaques (D) and circulatory NKG2D+ NK cells of low VL macaques (F). Data are shown as minimum to maximum floating bars with a horizontal line

representing the mean. *, $p<0.05$ and **, $p<0.01$ indicate statistically significant differences by Mann-Whitney *t* test. Spearman‘s correlation analysis was used to determine statistical significance in B, D and F.

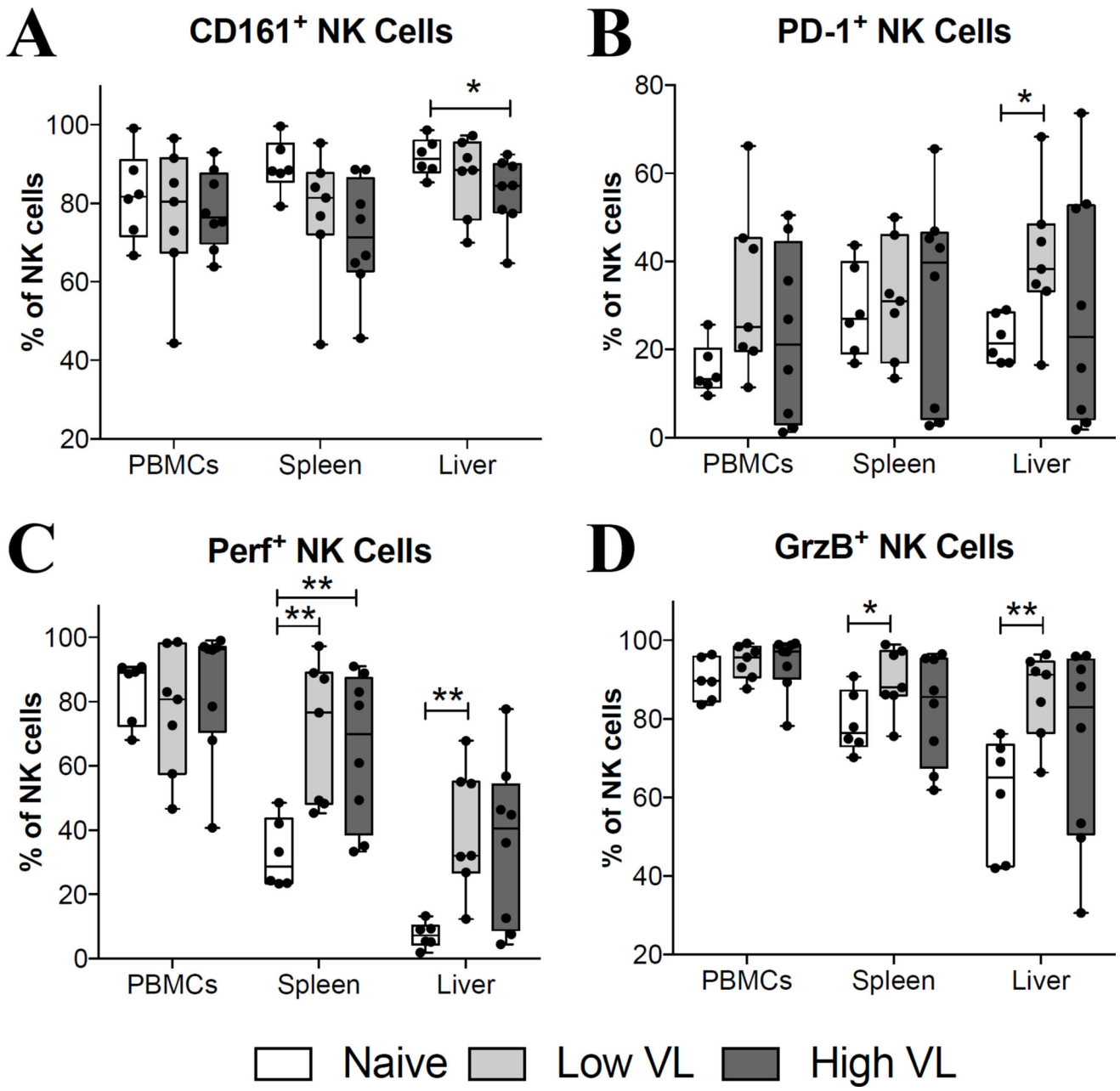

Fig. 4. SIV-infected macaques display increased expression of cytotoxic protein in spleen- and liver-resident NK cells

Lymphocyte single-cell suspensions were purified from blood, spleen and liver of SIV-negative (naïve) and SIV-infected (Low VL and High VL) macaques and stained fresh for flow cytometric analysis. (A–D) Expression of CD161 (A), PD-1 (B), perforin (C) and granzyme B (D) by circulatory and tissue-resident NK cells from naïve, low VL and high VL rhesus macaques. Data are shown as minimum to maximum floating bars with a horizontal line representing the mean. *, $p<0.05$ and **, $p<0.01$ indicate statistically significant differences by Mann-Whitney *t* test.

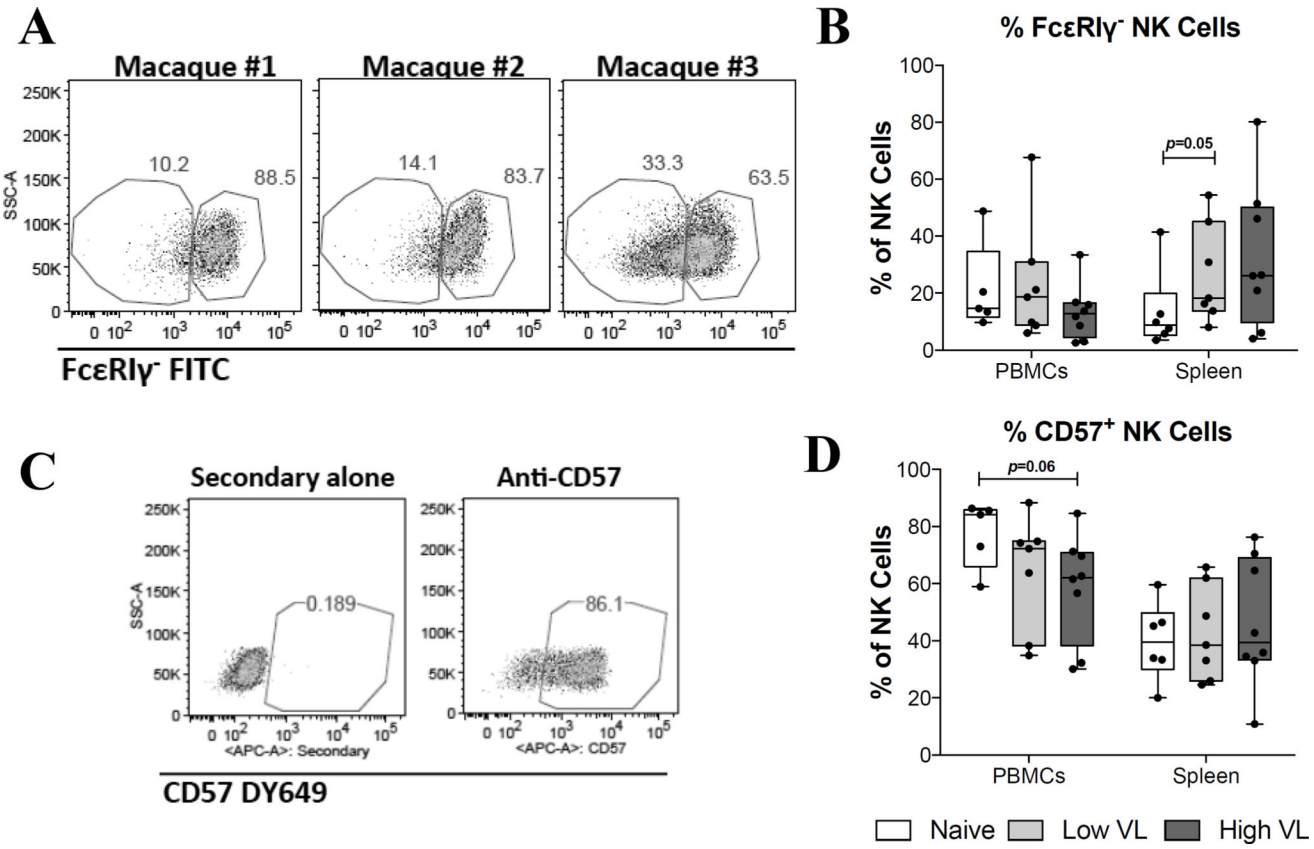

Fig. 5. SIV controlling macaques do not display accumulation of FcεRIγ-deficient or CD57$^+$ memory-like NK cells

Viably frozen single-cell PBMC and spleen samples from naïve, low VL and high VL rhesus macaques were thawed and stained for flow cytometric analysis. (A) Representative staining for FcεRIγ in rhesus PBMCs. (B) Deficiency in the adaptor protein FcεRIγ was evaluated by intracellular staining. (C) Representative staining for CD57 in rhesus macaque PBMCs. (D) Expression of CD57 on the surface of circulatory and splenic NK cells was determined using a purified monoclonal antibody followed by detection with a secondary DY649-conjugated antibody. Data are shown as minimum to maximum floating bars with a horizontal line representing the mean. p=0.05 as determined by Mann-Whitney t test.

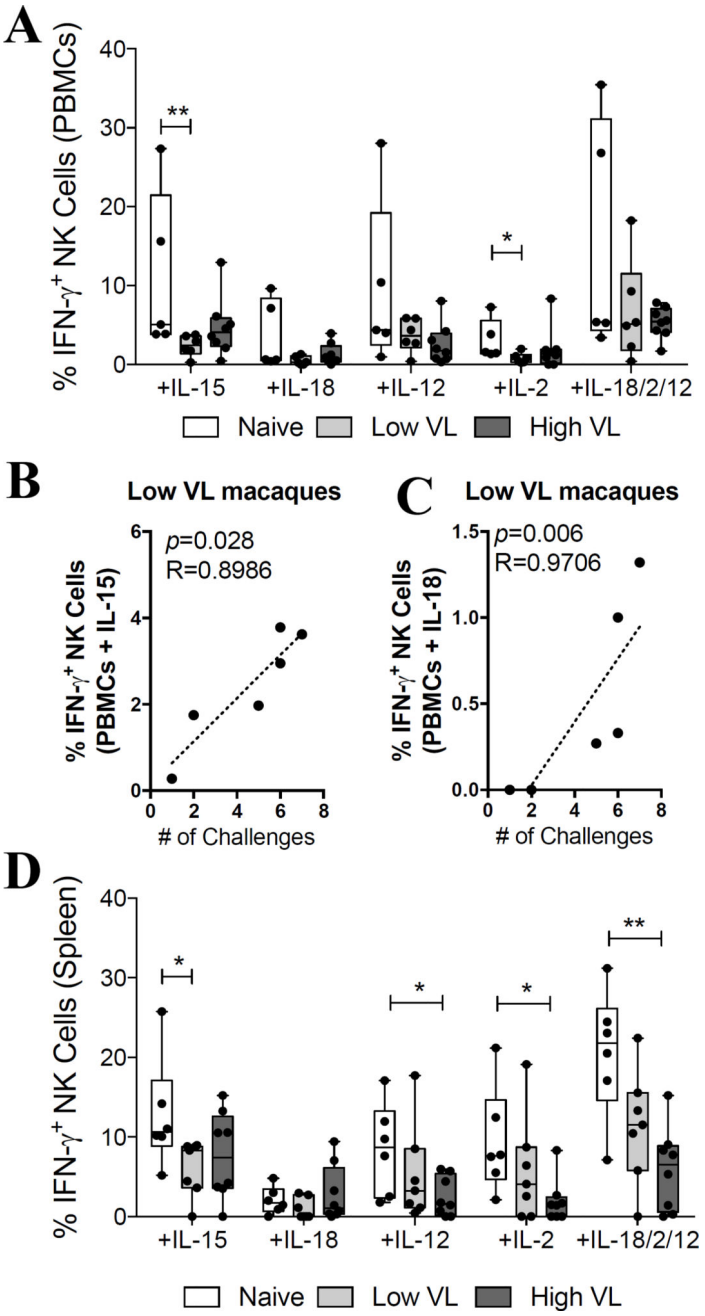

Fig. 6. Control of chronic viremia in SIV-controlling macaques is associated with NK cell activation by IL-15 and IL-18

Viably frozen single-cell PBMC and spleen samples from naïve, low VL and high VL rhesus macaques were thawed and stimulated with recombinant cytokines as described in materials and methods. (A) IFN-γ production by circulatory NK cells in response to stimulation with IL-15 (50 ng/ml), IL-18 (500 ng/ml), IL-12 (500 ng/ml), IL-2 (500 ng/ml) and IL-18+IL-12+IL-2 (500 ng/ml each). (B–C) Correlation between the number of challenges needed to acquire SIV_{mac251} infection and the proportion of IFN-γ^+ NK cells in response to IL-15 (B) and IL-18 (C) treatment. (D) IFN-γ production by circulatory NK cells in response to cytokine-dependent stimulation. Viably frozen PBMCs from low VL macaques

were only available from six animals. Data are shown as minimum to maximum floating bars with a horizontal line representing the mean. *, $p<0.05$ and **, $p<0.01$ indicate statistically significant differences by Mann-Whitney *t* test. Spearman's correlation analysis was used to determine statistical significance in B and C.

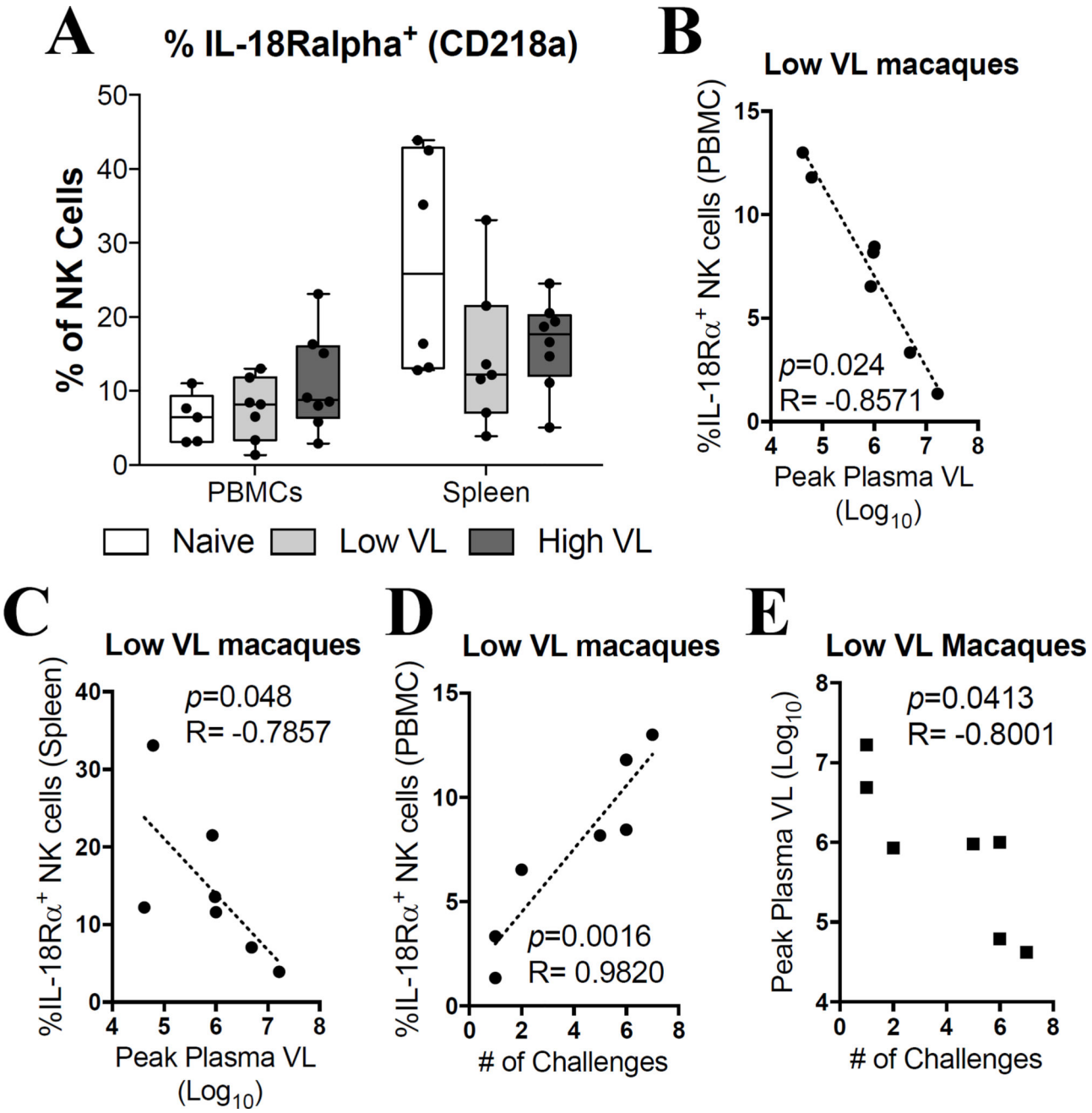

Fig. 7. Expression of IL-18Rα and IL-12Rβ1 by NK cells is associated with decreased peak plasma viral loads in SIV controlling macaques

Viably frozen single-cell PBMC and spleen samples from naïve, low VL and high VL rhesus macaques were thawed and stained for flow cytometric analysis. (A) Expression of IL-18Rα in circulatory and splenic NK cells. (B–C) Correlation between peak plasma viral loads and IL-18Rα expression by circulatory (B) and splenic (C) NK cells in low VL macaques. (D) Correlation between IL-18Rα expression in circulatory NK cells of low VL macaques and the number of challenges needed to acquire SIV_{mac251} infection. (E) Correlation between the peak viral load in low VL macaques and the number of challenges needed to acquire SIV_{mac251} infection. Data are shown as minimum to maximum floating bars with a

horizontal line representing the mean. Spearman‘s correlation analysis was used to determine statistical significance in B, C, D and E.

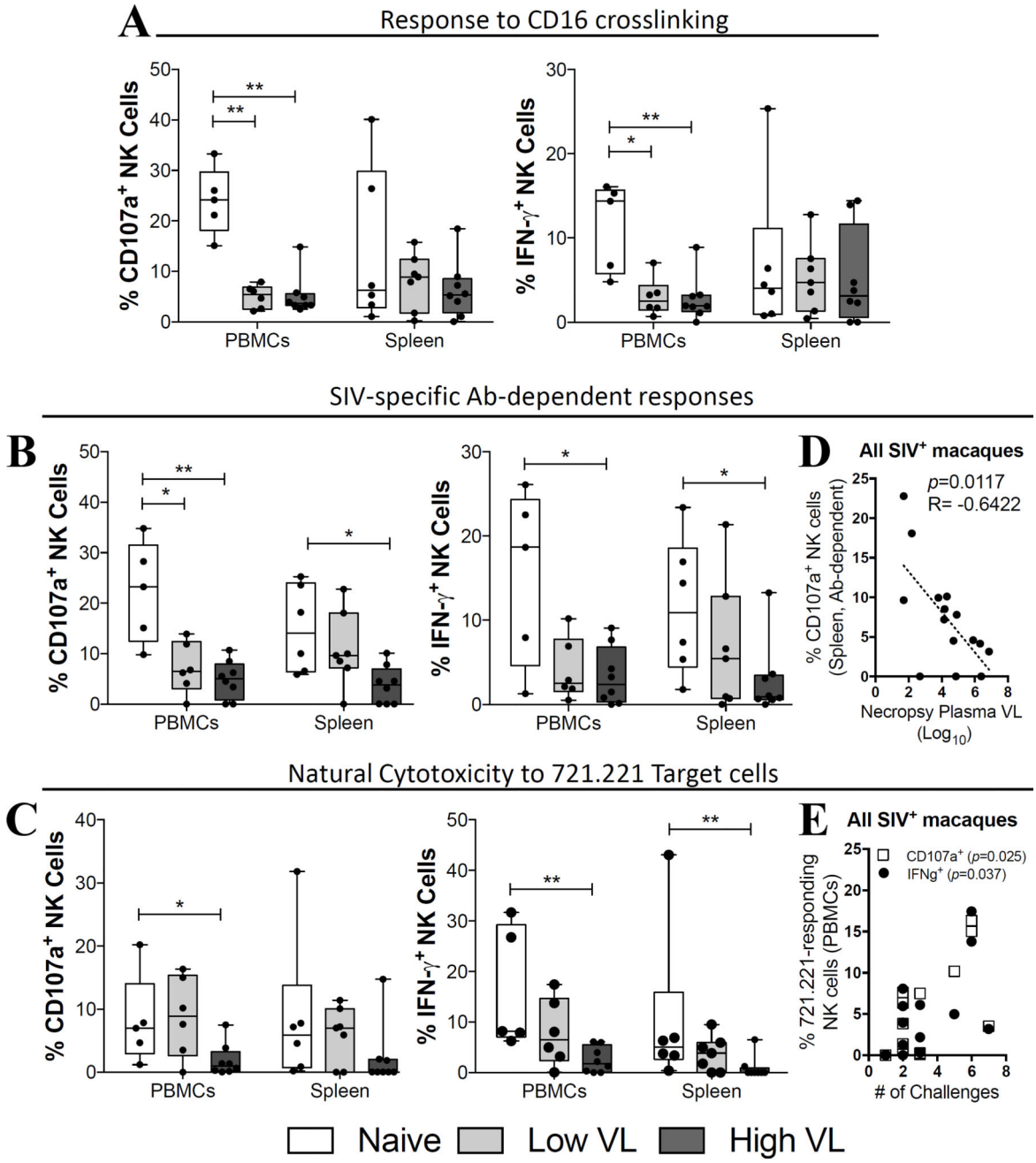

Fig. 8. Increased cytotoxic and antibody-dependent function are associated with lower viremia and delayed SIV acquisition in SIV controlling macaques

Viably frozen single-cell PBMC and spleen samples from naïve, low VL and high VL rhesus macaques were thawed and stimulated as described in materials and methods. (A–C) Cytotoxic (CD107a) and cytokine-producing (IFN-γ) activity in response to CD16 crosslinking (A), SIV-specific antibody-mediated activation (B) and co-culture with MHC-I-devoid 721.221 target cells (C). (D) Correlation between plasma viral loads at necropsy and antibody-dependent cytotoxic activity by splenic NK cells in all SIV-infected macaques. (E) Correlation between the number of challenges needed to acquire infection and the cytotoxic response to 721.221 target cells (IFN-γ and CD107a) by circulatory NK cells in all SIV-

infected macaques. Data are shown as minimum to maximum floating bars with a horizontal line representing the mean. *, $p<0.05$ and **, $p<0.01$ indicate statistically significant differences by Mann-Whitney *t* test. Spearman's correlation analysis was used to determine statistical significance in D and E.